RESEARCH ARTICLE ISSN: 2349-2678

Contents lists available at www.ijpba.in
International Journal of Pharmaceutical and Biological Science Archive
NLM (National Library of Medicine ID: 101732687)
Index Copernicus Value 2019: 71.05
Volume 9 Issue 4; July-August; 2021; Page No. 12-26

DESIGN OF DUAL ALLOSTERIC INHIBITORS OF B-RAF AND C-RAF KINASES FOR CANCER TREATMENT

Nicholas A. Nesh

Physics Department, The College of New Jersey, 2000 Pennington Road, Ewing, New Jersey, 08628 USA

E-mail neshn@tcnj.edu

Conflicts of Interest: Nil
Corresponding author: Nicholas A. Nesh
DOI: https://doi.org/10.32553/ijpba.v9i4.242

ABSTRACT

We present a computational design of new, druglike small molecules that could allosterically inhibit both B-Raf and C-Raf kinases. The Raf kinases stimulate activators of MAPK pathways. MAPK pathways participates in cell proliferation and apoptosis. Mutations of the proteins in the pathway have been implicated in cancers. Many cancer drugs are MAPK inhibitors (MAPKi). Although MAPKi decrease cancer growth, bypass signaling is often formed. Consequently, most patients develop MAPKi resistance within a year. Most kinase inhibitors bind to the kinase catalytic site. These sites are similar in many kinases, making it challenging to target them specifically. Allosteric sites differ between kinases, permitting selective binding. Catalytic-site B-Raf inhibitors can successfully restrain the kinase in cancers with mutated B-Raf. However, they also promote dimerization of B-Raf with either itself or C-Raf. This can increase the C-Raf activation if an upstream Raf-activator is mutated. A simultaneous inhibition of both B-Raf and C-Raf is needed to avoid the development of cancer treatment resistance. The Deep View program was used to analyze the B-Raf and C-Raf binding sites. New putative small-molecule inhibitors were designed by systematically modifying the known inhibitors. The DataWarrior and Molinspiration programs were used to calculate the druglike properties of the designed molecules. Molecules with optimal druglike properties and no indicated toxic risks were docked to B-Raf and C-Raf using the ArgusLab program. The binding energies of stable complexes were calculated. Three designed molecules had better druglike properties and bound allosterically both B-Raf and C-Raf with higher binding energies than known inhibitors did. Our work, coupled with prior experimental studies, suggest that the molecules designed here may be potent allosteric inhibitors of both B-Raf and C-Raf. They may achieve increased therapeutic response in tumors with either B-Raf mutations or mutations of upstream activators of Raf.

Keywords: Druglike Small Molecules, Allosteric Inhibitors, Raf Kinases.

Introduction

Chemotherapy treatments of many cancers fail due to patients developing drug resistance [1]. As many as 30% to 40% of cancer patients develop metastases, with a median survival of about two years [2, 3]. New, more effective anti-cancer drugs are essential for increasing the survival rates.

Apoptosis, or programmed cell death, is a natural process for eliminating injured cells [4]. Defective apoptotic pathways allow damaged cells to survive and become unresponsive to therapies, leading to uncontrolled cell growth and cancer advancement [5]. Designing molecules that can bypass damaged apoptotic

pathways is important for cancer treatments [6].

Cellular proteins can either promote cell death (proapoptotic) or inhibit it (antiapoptotic). An injured cell sends stress signals, which cause proapoptotic proteins to inactivate antiapoptotic ones, thus priming the cell for apoptosis [7]. Typically, this triggers a disintegration of the cell's mitochondrial membrane [8], leading to cell death. Damaged apoptotic pathways are often present in cancer cells [9]. Small molecules that can inhibit damaged cell cycle regulators have been used to treat cancers [10].
Research on protein kinases is important because of their roles in many cancers [11, 12]. Kinases are enzymes that are highly regulated and are essential for many cell functions, including metabolism, cell division, transcription, immune response, and apoptosis [13]. A kinase can modify the activity of a receptor protein by phosphorylating it on its serine, tyrosine, histidine, or threonine residues. The phosphorylation can either promote or prevent the receptor's interactions with other proteins [13].

When protein kinases interact with other proteins or small molecules, they can be activated or inhibited [14]. Most known kinase inhibitors bind with a high affinity to the catalytic site of a kinase [15, 16]. However, many kinases have very similar catalytic sites, which makes it difficult to target them selectively [17,18]. The selectivity is important, since molecules that indiscriminately inhibit several kinases may damage healthy tissue, leading to undesirable side effects in patients [19].

Recent trends in cancer drug discovery have been directed toward designing allosteric kinase inhibitors [20, 21]. An allosteric site of a kinase is structurally different from its catalytic site. While the effectiveness of ATP-competitive inhibitors greatly depends on the ATP concentration, an allosteric inhibitor can keep its inhibitory efficacy at various concentrations [22, 23]. Since allosteric sites differ among kinases, a highly specific binding can be achieved [24, 25]. Drugs that bind allosterically are likely to cause fewer side effects. So far, allosteric small molecule inhibitors have been found for a relatively small number of kinases [26, 27].

A Mitogen-Activated Protein Kinase (MAPK) pathway transfers signals from the cell's surface to the cell's nucleus [28]. A mutated protein in the MAPK pathway can get stuck in either an "on" or an "off" position, leading to cancer development [29]. Compounds that can unstuck such mutated proteins can be used for cancer therapies [30].

Kinases in a MAPK pathway participate in cell propagation and apoptosis. Many cancer drugs are MAPK inhibitors (called MAPKi) [29]. While MAPKi can slow cancer progression, bypass signaling is often established [31]. As a result, most patients acquire MAPKi resistance within a year.

A MAPK pathway is activated by a mitogen-activated protein kinase (MEK) kinase, while MEK kinases are activated by Raf kinases [30, 31]. The three Raf kinases, A-Raf, B-Raf, and C-Raf, are serine/threonine-specific kinases. They are highly regulated since they impact cellular growth and proliferation, [32]. Downstream, Raf kinases act on MEK1 and MEK2 kinases, which activate extracellular signal-regulated kinases ERK1 and ERK2 [31].

The Raf kinases are activated by Ras G-proteins, which communicate cell signals [31, 33]. An activated Ras protein turns on other proteins, which eventually leads to cell proliferation and survival. Mutations can create permanently activated Ras that can maintain cell signaling even in the absence of inducers. Since this signaling leads to cell growth and division, hyperactive Ras can result in cancer [34].

The development of resistance to cancer treatment relates to the paradoxical activation of MEK/ERK signaling [35], largely due to C-Raf activation [36, 37]. Mutated Ras cannot signal via B-Raf because that produces too much ERK signaling, which then leads to apoptosis [38]. Cancer cells with mutated Ras appear to switch their signaling from B-Raf to C-Raf since those

cause weaker ERK signaling. Previous studies showed that B-Raf is not needed for ERK activation in Ras-mutated cells. [37, 38]

Mutations in the Raf kinases, especially in B-Raf, have been found in many cancers [39], making B-Raf one of the main targets of cancer treatments [33]. In cancer cells with mutant B-Raf, catalytic-site inhibitors of B-Raf effectively constrain the kinase. However, they also promote dimerization of B-Raf with either itself or C-Raf. This, in turn, can boost C-Raf activation if an upstream Raf-activator is mutated. The creation of an alternate route via C-Raf can lead to resistance to cancer treatments [33]. Simultaneous inhibition of both B-Raf and C-Raf is needed to overcome the resistance [38].

Sorafenib is a drug that inhibits several kinases, including Raf [40, 41]. The drug is more selective for C-Raf than for B-Raf [42]. Sorafenib is used to treat some renal, liver, and thyroid cancers [43, 44]. Previous clinical trials showed that treatment with sorafenib leads to a considerable increase in disease-free survival, but not in overall patient survival rates [45]. Very often, sorafenib causes bothersome side effects [46].
Vemurafenib, a Raf inhibitor, is successful in treating melanomas with a specific B-Raf mutation [47]. However, about 40% of melanomas lack that mutation and are not arrested by the drug. Vemurafenib paradoxically stimulates non-mutated B-Raf and may enhance cancer progression in such cases [48].

PLX5568 is another drug used to treat a variety of cancers with overactive B-Raf. The drug prevents the cancer advancement by inhibiting defective regulators of cell proliferation [49]. PLX5568 binds to the catalytic site of B-Raf and, thus, is not selective to the kinase [50]. Clinical trials showed that resistance to PLX5568 develops within a few months, leading to cancer relapse [51].

Inhibitors PLX7904, PLX7922, and PLX8394 can defeat several known resistance mechanisms in cancers with B-Raf mutations [52]. PLX8394 is one of the more successful Raf inhibitors, called a paradox breaker. Nevertheless, a limited response to PLX8394 was observed in a clinical trial where tumor size decreased by at least 30% in about 22% of patients [53].

This research focuses on computational design of new, druglike small molecules that could bind to both B-Raf and C-Raf kinases at their allosteric sites and have better binding and druglike properties than the currently known inhibitors. This would be especially important in cancers with either B-Raf mutations or mutations of upstream activators of Raf [54].
To be suitable for drug development, a designed small molecule should be non-toxic and have metabolic stability, bioavailability, and transport properties comparable to those of known drugs. These characteristics are determined by molecular mass, hydrophilicity, aqueous solubility, electronic bond distributions, flexibility, polar surface area, and druglikeness [55, 56].

Molecules with a higher molecular mass are usually more active than those with a lower mass. However, such molecules are also less likely to be absorbed and, thus, less likely to reach their desired target. Consequently, the mass of a promising druglike molecule should be as low as possible without compromising its effectiveness. More than 80 % of known drugs have a molecular mass less than 450 g/mol [57].

The value of the logarithm of the partition coefficient between n-octanol and water, or logP, can reliably predict molecule's hydrophilicity [56]. A low logP value corresponds to high hydrophilicity. A study of more than 3000 known drugs found out that a molecule must have a value of logP ≤ 5 to be well absorbed [56].

The aqueous solubility of a molecule significantly affects its absorption. In general, good absorption is indicated by a high value of logS (logarithm of the solubility measured in mol/liter). Over 80% of existing drugs have logS greater than - 4, which corresponds to a

solubility of 0.1 mmol/liter [56, 55]. For most known drugs -4 < logS < 1 [56].

The total surface area of all polar atoms in a molecule is called the polar surface area (PSA). A PSA value is a good predictor of the molecule's bioavailability, including its ability to penetrate blood-brain barrier and cell membranes in intestinal walls [58]. A PSA value of most available drugs is less than 90 $Å^2$ [59]. Molecules with greater PSA values usually have reduced bioavailability. Oral bioavailability of a molecule is also affected by its flexibility [60]. The flexibility depends on the molecule's number of rotatable bonds. As shown previously [61], molecules with 10 or fewer rotatable bonds and fewer than 6 hydrogen bond donors show good oral bioavailability [61].

The goal of this work was to computationally design new, druglike small molecules that would simultaneously bind B-Raf and C-Raf at their allosteric sites, thus potentially promoting apoptosis in cancer cells.

Methods

Computational Tools:

The following computational tools were used to design and evaluate putative small molecule inhibitors of B-Raf and C-Raf kinases: Protein Data Bank [62], Deep View [63], ArgusLab [64], Molinspiration [65], and Osiris DataWarrior [57].

The Protein Data Bank (PDB) [62] is an international database that provides experimentally determined, three-dimensional structures of both single molecules and small molecules bound to larger ones. The DeepView program [63] allows a visualization of molecular structures obtained from the PDB. Atomic distances, H-bonds, angles, and charge densities can be studied in DeepView. The program can also compare the structures of active sites by overlaying several kinases simultaneously.

The ArgusLab program [64] uses PDB kinase structures to view and study their binding sites, conduct docking simulations, and find optimal properties of docked molecules. The Molinspiration program [65] can be used to study molecular rotatable bonds and H-bond donors, both of which help determine the drug-like properties of designed molecules.

The DataWarrior program [57] can evaluate designed molecules for possible toxicities, as well as for tumorigenic, mutagenic, reproductive, or irritational risks. A molecule could still carry risks, even if DataWarrior does not indicate any. However, DataWarrior has been shown to be a dependable predictive tool [66]. For example, when evaluated on a group of compounds with known mutagenicities, the program correctly recognized 86% of them as mutagenic. On the other hand, it implicated as possibly mutagenic only 14% of known drugs from a control group [57]. Likewise, DataWarrior correctly flagged as toxic 86% of tested compounds with known risks, while identified only 8% of the known drugs as having such risks. A druglikeness score is an important molecular property computed by DataWarrior. The methods and validation studies used to obtain the score are explained in detail elsewhere [57]. A positive value of the druglikeness score suggests that a molecule is mainly comprised of fragments usually found in known drugs.

No single attribute can ensure that a designed molecule will be a good drug candidate. However, a favorable set of druglike properties and no implied risks can indicate a molecule that merits further experimental investigation. The DataWarrior program [57] uses the molecule's mass, the logS and logP values, the druglikeness, and toxicity assessments to compute the molecule's overall Drug Score. The Drug Score, which can have values between 0 to 1, is used to assess a molecule's overall drug potential [57]. The grater the Drug Score value, the likelier it is for a molecule to be biologically active and non-toxic. This technique efficiently distinguishes between promising drug candidates and inactive

molecular structures [66].

Dataset:

The three-dimensional structure of B-Raf bound to PLX7922 (PDB ID 4XV3) was downloaded from the Protein Data Bank [62]. The PLX7922 was bound in the allosteric site of B-Raf. Similarly, the three-dimensional structure of the C-Raf-kinases was downloaded from the Protein Data Bank, PDB ID 3OMV [62], as well as the structure of PLX8394 [52].

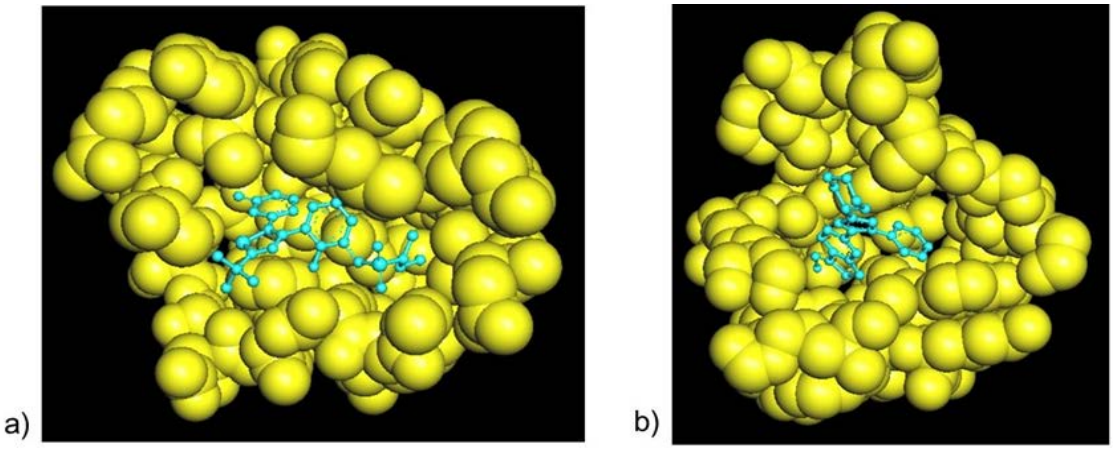

Figure 1 a) B-Raf allosteric pocket showing the residues (yellow balls) within an 8.0 Å radius from the PLX7922 ligand (blue ball-and-stick). b) C-Raf allosteric pocket showing the residues (yellow balls) within an 8.0 Å radius from its ligand (blue ball-and-stick). To improve visibility, the front-facing B-Raf and C-Raf residues were removed.

Fig. 1 a) shows the allosteric site of B-Raf bound to its experimentally known allosteric small-molecule inhibitor, PLX7922 (blue) [63]. Only the B-Raf residues within an 8.0 Å radius from PLX7922 are shown. Fig. 1 b) shows a ligand bound to the allosteric site of the C-Raf kinase. Again, only the C-Raf residues within an 8.0 Å radius from the ligand are shown.

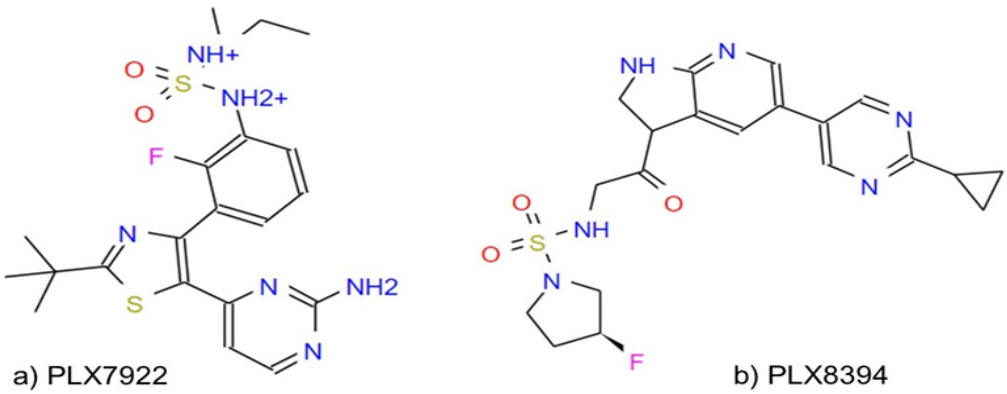

Figure 2 The structures of allosteric B-Raf inhibitors a) PLX7922 and b) PLX8394

Fig. 2 shows the structures of the known allosteric B-Raf inhibitors (the, so called, paradox breakers), PLX7922 and PLX8394 [62]. We can see that both molecules contain benzene rings, imidazole groups, and a high number of nitrogen atoms. The cyclic groups improve the stability and the binding properties of the molecules, while the absence of heavy atoms increases their biologically solubility. The information obtained from the structures of these inhibitors was used to design novel small molecule that could potentially simultaneously bind B-Raf and C-Raf-at their allosteric sites.

Procedure Employed:

The three-dimensional structures of the known inhibitors, PLX7922 and PLX8394, were uploaded and then analyzed using the DataWarrior program [57]. The following properties were determined: molecular mass, hydrophilicity, aqueous solubility, electronic bond distributions, polar surface area, flexibility, druglikeness, toxic risks, and the total Drug Score. At the end, these values were compared to the properties of new molecules designed here.

Next, the structures of B-Raf, PLX7922, and PLX8394 were uploaded in ArgusLab [64] and the inhibitors docked into B-Raf. The goal was to find the binding energy of each inhibitor in the allosteric site, as found by ArgusLab, and compare those values to the binding energies of the newly designed molecules in complex with each of B-Raf and C-Raf.

The structures of PLX7922 and PLX8394 were used as initial templates to design new molecules that could simultaneously bind B-Raf and C-Raf at their allosteric sites. Over thirty trial molecules were designed by making systematic atomic substitutions in the known inhibitors. The substitutions were carefully chosen to enhance the molecule's druglike properties without reducing the desirable characteristics of the inhibitors.

DataWarrior [57] and Molinspiration [65] were used to find the mass, solubility, the logP value, the number of rotatable bonds, and the number of hydrogen bond donors for each newly designed molecule. DataWarrior also searched for any toxicities and mutagenicities. The total Drug Score was calculated for each molecule. The findings were then used to iteratively design new small molecules with improved druglike properties.

Designed small molecules with optimal druglike characteristics and no implied risks, were then used for the docking studies. Their three-dimensional structures were reconstructed and optimized in ArgusLab. The Semiempirical Geometry Optimization and Molecule Builder functions [64] were used. Then, the designed molecules were separately docked into B-Raf and C-Raf using the ArgusDock function. Molecular bond rotations were allowed during the docking. The AScore scoring function, a 0.4 Å grid resolution, and ascore.prm parameter set were used [64]. ArgusLab determined the binding energies of the stable complexes of B-Raf and C-Raf with each of the designed molecules. The more negative the binding energy, the stronger the affinity between the kinase and the molecule. The main goal was to achieve an allosteric binding between the molecules and each kinase, while improving the overall druglike properties of the molecules.

Results Design of Putative Small Molecule Inhibitors:

Druglike properties of the known B-Raf inhibitors, PLX7922 and PLX8394, were calculated using the DataWarrior [57] and Molinspiration [65] programs. The goal was to determine these values for the known inhibitors and then compare them to those of newly designed molecules. The findings are presented in Table 1.

Table 1: Druglike properties of PLX7922 and PLX8394

Inhibitor	logP	logS	PSA ($Å^2$)	MM (g/mol)	Rotatable bonds	H-acceptors	H-donors	Drug Likeness	Drug Score[b)]
PLX7922	2.7	-6.7	130	513	7	9	2	3.0	0.39
PLX8394	2.8	-7.2	129	543	7	9	2	3.7	0.35

[a)] *MM= molecular mass*

[b)] *obtained using a DataWarrior macro routine* [57]

As shown in Table 1, both PLX7922 and PLX8394 had fewer than 10 rotatable bonds and fewer than 6 H-bond donors. These values were in the desired range for druglike

molecules. Also, the logP values were below 5, which indicated that the drugs were well absorbed. As expected, neither PLX7922 nor PLX8394 showed any irritant, mutagenic, tumorigenic, or reproductive effects, as found by both DataWarrior and Molinspiration.

However, the PSA value of both molecules was greater than 90 $Å^2$, showing that the molecules likely have a lower bioavailability than most of the known drugs. Both molecular mass values were greater than 450 g/mol, which implies increased activity, but also a somewhat reduced absorptivity. The values of logS for both PLX7922 and PLX8394 were much lower than a minimum desired value of -4. This indicates a lower solubility than is typical for most drugs. The overall Drug Score for each of the known inhibitors were less than 0.40.

We analyzed the structures of PLX7922 and PLX8394, concentrating on their similarities and differences. To obtain molecules with improved druglike properties we did systematic atomic substitutions and added or removed the ring structures. This allowed us to iteratively design several promising new small molecules that could potentially bind allosterically to both B-Raf and C-Raf. Three molecules with the best druglike properties and highest binding energies are shown in Fig. 3.

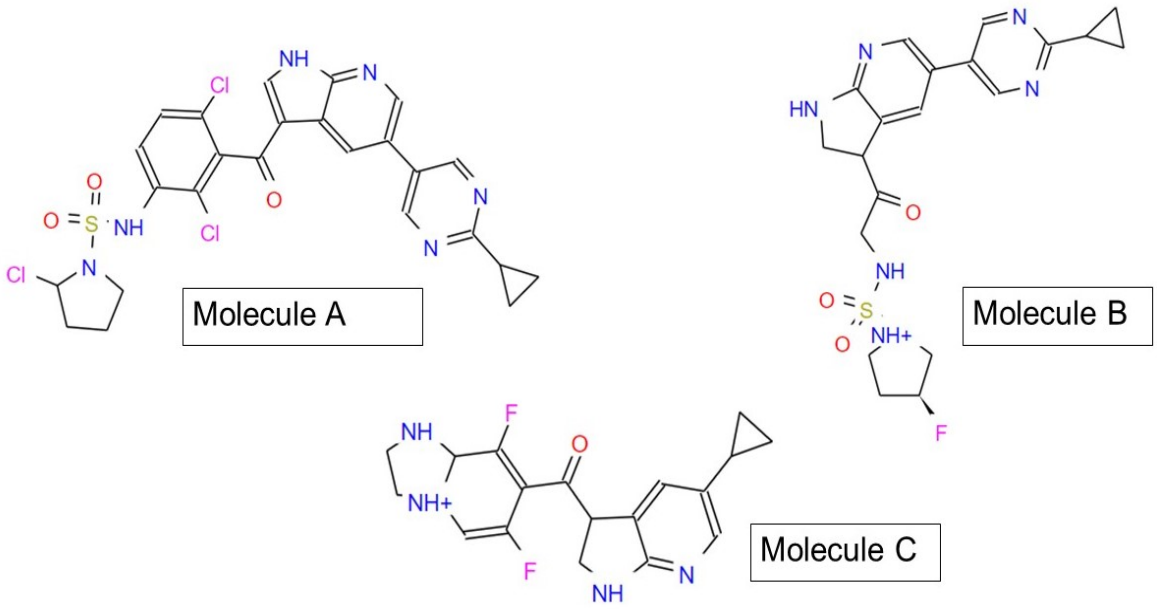

Figure 3: The structures of the designed molecules, A, B, and C, found to have the best druglike properties and that formed the most stable complexes with B-Raf and C-Raf.

Evaluation of Druglike Properties:

The DataWarrior and Molinspiration programs were used to calculate the druglike properties of the designed molecules. The three designed molecules in Fig. 3 had the best overall druglike properties. They also had no indicated irritant, mutagenic, tumorigenic, or reproductive risks. Their chemical compositions were: $C_{25}H_{21}N_6O_3Cl_3S$ (molecule A); $C_{20}H_{23}N_6O_3FS$ (molecule B), and $C_{18}H_{19}N_4OF_2$ (molecule C).

The logP and logS values, the PSA values, the molar masses (MM), and the Drug Likeness were calculated using DataWarrior and Molinspiration. Comparable values were found by both programs. The number of rotatable bonds, H-bond donors, and H-bond acceptors were found using Molinspiration. A DataWarrior macro routine [**Error! Bookmark not defined.**] was used to obtain the Drug Score.

Table 2 shows the properties of molecules A, B, and C, as determined by DataWarrior and

Molinspiration. The letters A, B, and C associated with the molecules in Table 2 match those assigned to the molecules in Fig. 3.

Table 2: Druglike properties of designed molecules A, B, and C

Molecule	logP	logS	PSA (Å^2)	MM (g/mol)	Rotatable bonds	H-acceptors	H-donors	Drug Likeness	Drug Score[b)]
A	5.0	-4.4	128	591	7	9	2	4.3	0.71
B	1.2	-3.5	117	446	7	9	2	3.6	0.73
C	0.19	-3.9	57.3	344	3	5	3	3.5	0.79

[a)] *MM= molecular mass*
[b)] *obtained using a DataWarrior macro routine* [**Error! Bookmark not defined.**]

Like most known drugs, the three designed molecules had the logP value of 5.0 or less. Their logS values ranged from -3.5 to -4.4, as they do for a great majority of known drugs. These values were closer to the optimal drug range than were the logS values of the known inhibitors, PLX7922 and PLX8394 (see Table 1).

The polar surface area (PSA) of molecule C was 57.3 Å^2. This was substantially below a typical value of 90 Å^2 for commercial drugs. The PSA values of molecules A and B were 128 Å^2 and 117 Å^2, respectively. These values, which are close to the approximate range of known drugs, were slightly lower than those for PLX7922 and PLX8394, indicating better bioavailability. The molar mass (MM) of molecule A was 591 kJ/mol, which was comparable to the molar masses of the known inhibitors. The molar mass of molecule B was less than 450 g/mol, while that of molecule C was less than 350 g/mol. These molar masses were in the range of molecular masses of more than 80 % of known drugs.

The number of rotatable bonds, H-bond acceptors, and H-bond donors also suggest good oral bioavailability. This is especially true for Molecule C which had only 3 rotatable bonds, 5 H-bond acceptors, and 3 H-bond donors. All three molecules had druglikeness values between 3.5 and 4.3. These values were higher than those for PLX7922 and PLX8394. As discussed in the Introduction section, these values should reliably predict the overall drug potential of the designed molecules [57, 58, 61].

The Drug Score values were 0.71 for molecule A, 0.73 for molecule B, and 0.79 for molecule C. These values were about two times greater than those of the known inhibitors PLX7922 and PLX8394. As we said before, Drug Score values can range between 0 to 1 and are used to assess molecules' overall drug potential [57]. The greater the score, the likelier that the molecule will be biologically active and non-toxic [65].

Allosteric Binding of Designed Molecules:

To establish reference values, the known allosteric inhibitors, PLX7922 and PLX8394, were docked in B-Raf and C-Raf using the ArgusLab program. The properties of the B-Raf and C-Raf allosteric binding sites were also analyzed. As shown in Table 3, the binding energy of PLX7922 with B-Raf was -36.8 kJ/mol and with C-Raf it was -39.3 kJ/mol. The binding energies of PLX8394 were -33.1 kJ/mol and -34.3 kJ/mol with B-Raf and C-Raf, respectively. A more negative binding energy indicates a stronger bond and a higher affinity between the inhibitor and the kinase.

Next, the designed molecules were docked to B-Raf and C-Raf in ArgusLab. The binding energies of the molecules A, B, and C to B-Raf and C-Raf are given in Table 3. Molecule A formed the most stable bonds with both B-Raf and C-Raf, binding each of them allosterically with energies of -46.0 kJ/mol and -41.0 kJ/mol, respectively. These values are, respectively, about 19 % and 39 % more negative than those for PLX7922 and PLX8394, indicated a greater

affinity of the B-Raf and C-Raf kinases to molecule A, than to either of the known inhibitors. The binding energies of molecules B and C to B-Raf or C-Raf were between -35.0 kJ/mol and -36.6 kJ/mol. These values were similar to those between PLX7922 and PLX8394 and B-Raf and C-Raf.

Table 3: The Binding Energies of B-Raf and C-Raf and the Designed Molecules Compared to the Binding Energies of B-Raf and C-Raf with PLX7922 and PLX8394

Designed Molecule	B-Raf (kJ/mol)	C-Raf (kJ/mol)
A	-46.0	-41.0
B	-35.1	-35.0
C	-36.0	-36.6
PLX7922	-36.8	-39.3
PLX8394	-33.1	-34.3

Therefore, molecule A could bind allosterically to both kinases with an increased affinity and improved drug-like properties compared to the known inhibitors. For these reasons, molecule A was selected for further analyses of its allosteric binding to B-Raf and C-Raf. The analyses were done in the ArgusLab program.

Fig. 4 shows molecule A (green ball-and-stick) bound in the allosteric pocket of B-Raf (dark gray balls). The rest of the B-Raf molecules within a 5 Å radius from the ligand is also shown (light gray balls). For comparison, the PLX8394 inhibitor (pink ball-and-stick) is also shown bound to the allosteric pocket of B-Raf.

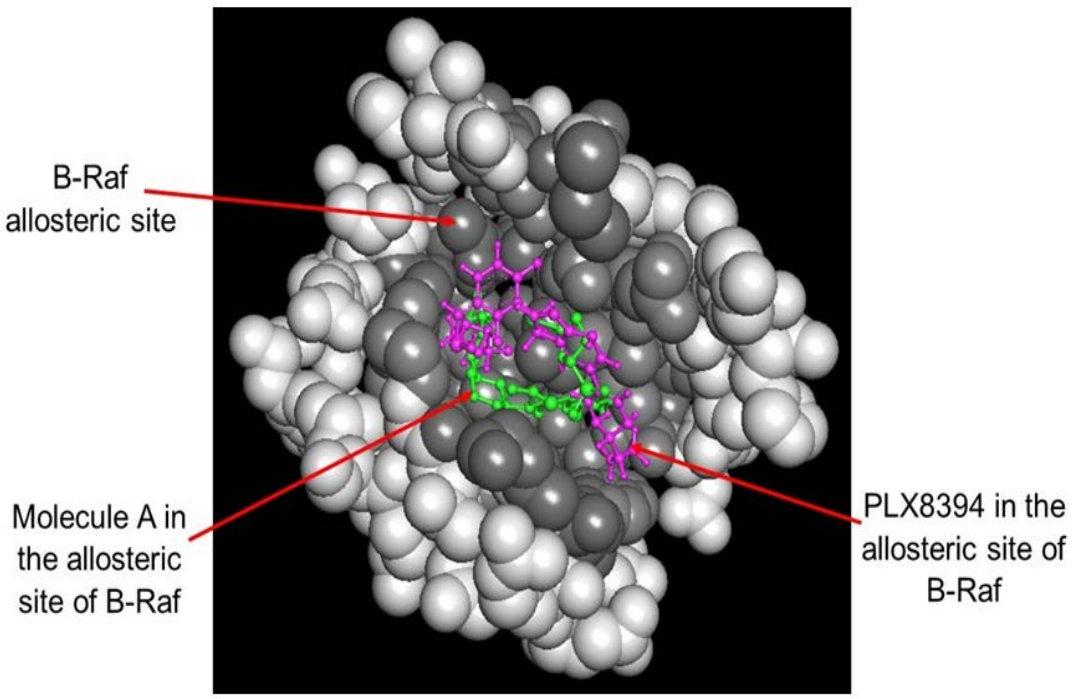

Figure 4 The designed molecule A (green ball-and-stick) is bound in the allosteric site of B-Raf (dark gray balls). The rest of the B-Raf molecule within a 5 Å radius from the ligand is also shown (light gray balls). For reference, PLX8394 (pink ball-and-stick) is also shown bound to the B-Raf allosteric pocket. To improve visibility, the front-facing B-Raf residues were removed.

The binding environment of molecule A docked in B-Raf was next analyzed in ArgusLab. The B-Raf residues within a 3-Å radius from molecule A were: Phe-468, Val-482, Leu-505, Leu-515, Leu-528, Trp-531, Asn-581, Asn-580, and Ile-592 (Fig. 5). All but two of these residues were non-polar and likely stabilized the ligand through van der Waals and hydrophobic interactions.

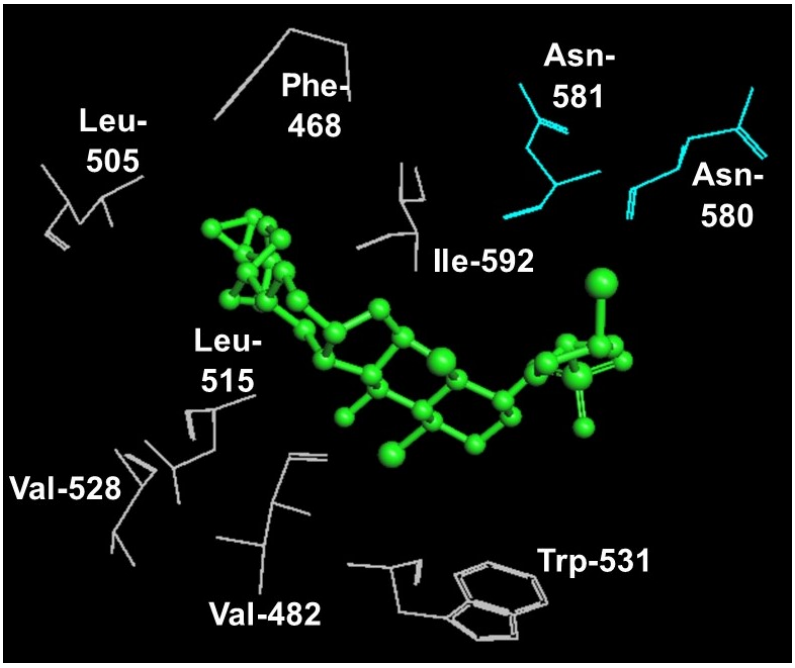

Figure 5 B-Raf residues within a radius of 3 Å from molecule A (green ball-and-stick). The molecules are orientated for optimized visibility. Gray = non-polar; blue = basic residues.

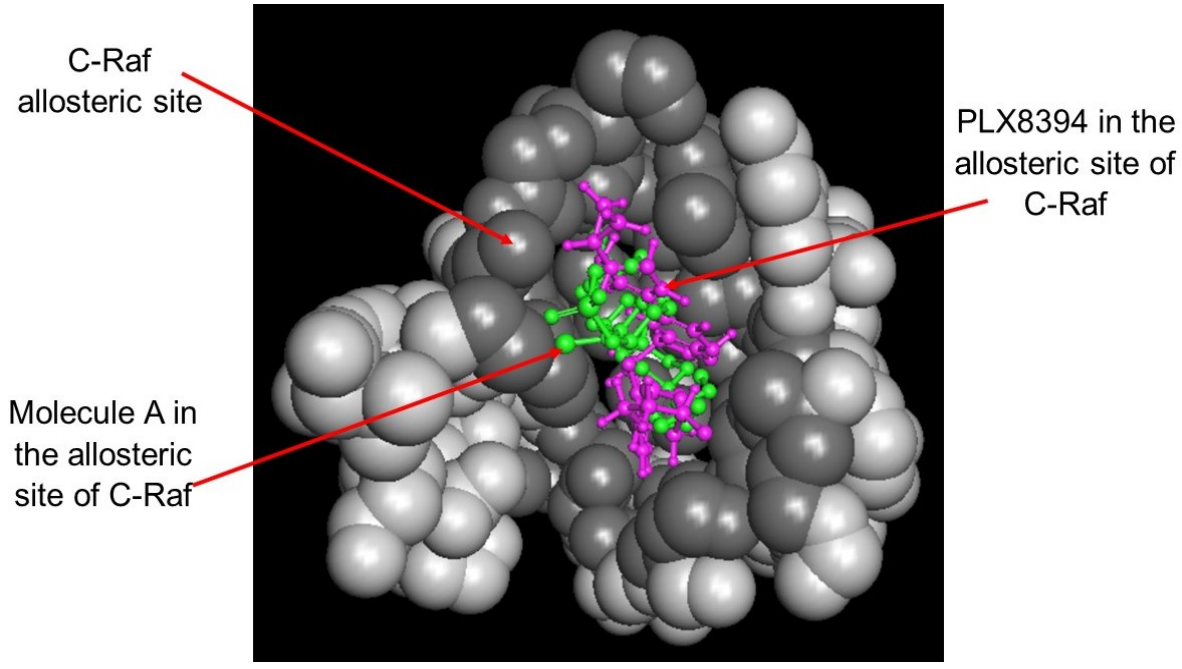

Figure 6 The designed molecule A (green ball-and-stick) is bound in the allosteric site of C-Raf (dark gray balls). The rest of the C-Raf molecules within a 5 Å radius from the ligand are also shown (light gray balls). For reference, PLX8394 (pink ball-and-stick) is also shown bound to the C-Raf allosteric pocket. To improve visibility, the front-facing C-Raf residues were removed.

Next, molecule A (green ball-and-stick in Fig. 6) was docked in C-Raf (gray balls), where it bound in the allosteric pocket (dark gray) with a binding energy of -41.0 kJ/mol. For comparison, the PLX8394 inhibitor (pink ball-and-stick) is also shown bound to the allosteric site of C-Raf.

In Fig. 7, we show the C-Raf residues within a radius of 3.5 Å from molecule A (green ball-and-stick): Val 363, Ala 373, Leu 406, Trp 423, Cys 424, Gly 426, Ser 427, and Phe 475 (Fig. 7). Five of these residues, Val 363, Ala 373, Leu 406, Trp 423, and Phe 475 are non-polar. They interact through hydrophobic and van der Waals forces and likely stabilize the binding of molecule A in the allosteric pocket.

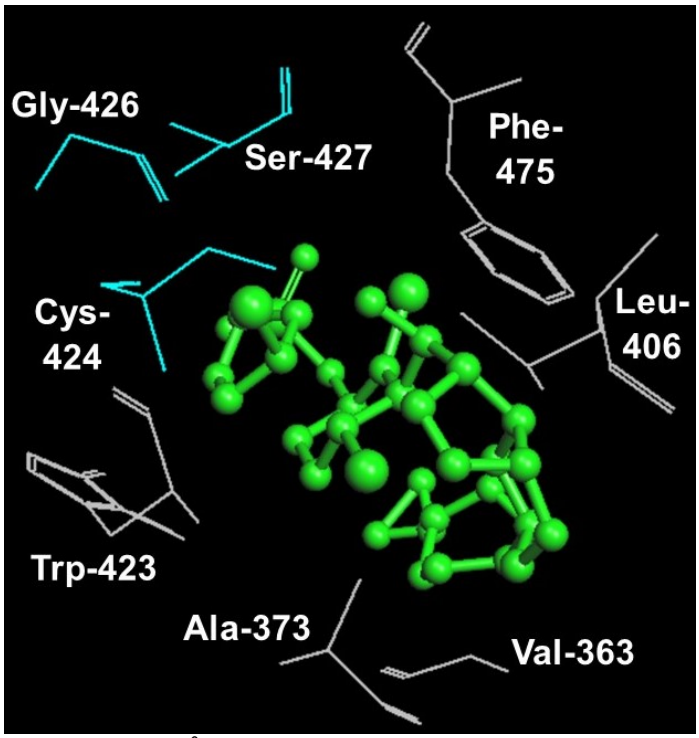

Figure 7 C-Raf residues within 3.5 Å from molecule A (green ball-and-stick). The molecules are oriented to optimize visibility. Gray = non-polar; blue = basic residues.

Discussion

We present computational design of putative simultaneous inhibitors of the B-Raf and C-Raf kinases at their allosteric sites. Three designed molecules that had optimal druglike properties and no known toxicities merited further analysis. The molar mass of molecule A was comparable to the molar masses of the known inhibitors, PLX7922 and PLX8394. The designed molecules B and C had the molar masses less than 450 kJ/mol and 350 g/mol, respectively. The three molecules also had logP values of 5 or less, 3 or fewer hydrogen bond donors, 9 or fewer H-bond acceptors, and 7 or fewer rotatable bonds.

The PSA and logS values of the designed molecules were comparable to those of the known drugs. They also had positive values of druglikeness and showed no toxic, mutagenic, or reproductive risks. The designed molecules also had about two times greater Drug Score values than PLX7922 and PLX8394 did. Such set of properties has been shown to reliably predict overall drug potential and a high likelihood that the molecules would be biologically active [66].

Especially promising is molecule A, which formed the most stable complexes with both B-Raf and C-Raf, binding each of them allosterically with energies of -46.0 kJ/mol and -41.0 kJ/mol, respectively. These binding energies were between 19 % to 39 % more negative than those for PLX7922 and PLX8394. Molecules B and C also had druglike properties that favorably compared to those of the known

inhibitors.

All three designed molecules made stable bonds with B-Raf and C-Raf during *in silico* docking. Their anticancer effectiveness ultimately needs to be evaluated *in vitro* and, if warranted, *in vivo*. While the syntheses of the molecules were not done, it should be noted that all three molecules were designed using the templates of the known B-Raf inhibitors. All three molecules bonded at the same allosteric sites where PLX7922 and PLX 8394 also bonded. Additionally, they had druglike characteristics similar to or better than PLX7922 and PLX 8394. Molecule B, especially, formed more stable complexes with B-Raf and C-Raf than the known inhibitors.

These results, combined with prior experimental and clinical studies of known B-Raf and C-Raf inhibitors, indicate that the molecules designed here may be very suitable candidates for simultaneous allosteric inhibition of both B-Raf and C-Raf. The simultaneous inhibition would lead to fewer side effects. They should also be especially valuable for preventing the development of drug resistance in cancers with either B-Raf mutations or mutations of upstream activators of Raf.

References

1. Housman G, Byler S, Heerboth S, et al. Drug Resistance in Cancer: An Overview. Cancers (Basel) 2014; 6(3): 1769–1792.
2. Mundy GR. Metastasis: Metastasis to bone: causes, consequences and therapeutic opportunities. Nature Reviews Cancer 2002; 2: 584-593.
3. O'Shaughnessy J. Extending Survival with Chemotherapy in Metastatic Breast Cancer. The Oncologist 2005; 10 (Suppl 3): 20-29.
4. Vaux DL, Cory S, Adams JM. Bcl-2 gene promotes haemopoietic cell survival and cooperates with c-myc to immortalize pre-B cells. *Nature* 1988; 33, 440.
5. Campos L, Rouault JP, Sabido O. High expression of bcl-2 protein in acute myeloid leukemia cells is associated with poor response to chemotherapy. *Blood* 1993; 81, 3091.
6. Barr FA, Sillje HH, Nigg EA. Polo-like kinases and the orchestration of cell division. *Nat Rev Mol Cell Biol* 2004; 5, 429.
7. Letai A, Bassik MC, Walensky LD, et al. Distinct BH3 domains either sensitize or activate mitochondrial apoptosis, serving as prototype cancer therapeutics. *Cancer Cell* 2002; 2, 183.
8. Chipuk JE, Kuwana T, Bouchier-Hayes L. Direct activation of Bax by p53 mediates mitochondrial membrane permeabilization and apoptosis. *Science* 2004; 303(5660):1010.
9. Lowery DM, Lim D, Yaffe MB. Structure and function of Polo-like kinases. *Oncogene* 2005; 24:248.
10. Barr FA, Sillje HH, Nigg EA. Polo-like kinases and the orchestration of cell division. Nat Rev Mol Cell Biol. 2004; 5: 429-440.
11. Kothe M, Kohls D, Low S et al. Structure of the Catalytic Domain of Human Polo-like Kinase 1. Biochemistry 2007; 46 (20) 5960–5971.
12. Wang F, Osawa T, Tsuchida R et al. Downregulation of receptor for activated C-kinase 1 (RACK1) suppresses tumor growth by inhibiting tumor cell proliferation and tumor-associated angiogenesis. Cancer Science 2011; 102: 2007–2013.
13. Manning G, Whyte DB, Martinez R et al. The protein kinase complement of the human genome. Science 2002; 298 (5600): 1912–34. doi:10.1126/science.1075762
14. Zhang J, Yang P, Gray N. Targeting cancer with small molecule kinase inhibitors. Nat Rev Cancer 2009; 9(1), 28.
15. Grover AK. Use of Allosteric Targets in the Discovery of Safer Drugs. Med Princ Pract. 2013 ; 22: 418–426
16. Huang D, Zhou T, Lafleur K et al. Kinase selectivity potential for inhibitors targeting the ATP binding site: a network analysis. *Bioinformatics* 2010; 26 (2), 198.
17. Hanks SK. Genomic analysis of the eukaryotic protein kinase superfamily: a

perspective. Genome Biol 2003; 4 (5): 111.
18. Hanks SK, Hunter T. Protein kinases 6. The eukaryotic protein kinase superfamily: kinase (catalytic) domain structure and classification. FASEB J 1995; 9 (8): 576–596.
19. Grunwald V, Heinzer H, Fiedler W. Managing side effects of angiogenesis inhibitors in renal cell carcinoma. Onkologie 2007; 30: 519–524.
20. Mandal S, Moudgil M, Mandal S. Rational drug design. Eur J Pharm 2009; 625: 90–100.
21. Wilhelm A, Lopez-Garcia LA, Busschots K et al. 2-(3-Oxo-1,3-diphenylpropyl)malonic acids as potent allosteric ligands of the PIF pocket of phosphoinositide-dependent kinase-1 development and prodrug concept. J Med Chem 2012; 55: 9817–9830.
22. Eathiraj S, Palma R, Hirschi M et al. A Novel Mode of Protein Kinase Inhibition Exploiting Hydrophobic Motifs of Autoinhibited Kinases. J Biol Chem. 2011; 286(23): 20677–20687.
23. Tan X, Osmulski PA, Gaczynska M. Allosteric regulators of the proteasome: potential drugs and a novel approach for drug design. Curr Med Chem 2006; 13: 155–165.
24. Hindie V, Lopez-Garcia LA, Biondi RM. Use of a fluorescent ATP analog to probe the allosteric conformational change in the active site of the protein kinase PDK1. Methods Mol Biol 2012; 928: 133–141.
25. Brognard J, Clark AS, Ni Y et al. Akt/protein kinase B is constitutively active in non-small cell lung cancer cells and promotes cellular survival and resistance to chemotherapy and radiation. Cancer Res. 2001; 61: 3986–3997.
26. Kim D-J, Choi C-K, Lee C-S et al. Small molecules that allosterically inhibit p21-activated kinase activity by binding to the regulatory p21-binding domain. Experimental & Molecular Medicine 2016; 48(4):e229-. doi:10.1038/emm.2016.13.
27. Amgalan D, Garner TP, Pekson R, et al. A small-molecule allosteric inhibitor of BAX protects against doxorubicin-induced cardiomyopathy. Nat Cancer 2020; 1(3):315-328.
28. Pongali R, Thammineni P. Cellular and Molecular Diagnostics. In: Advances in Cell and Molecular Diagnostics. 2018: p. 1-32.
29. Orton RJ, Sturm OE, Vyshemirsky V, et al. Computational modelling of the receptor-tyrosine-kinase-activated MAPK pathway. The Biochemical J. 2005; 392 (Pt 2): 249–61.
30. Sebolt-Leopold JS. Advances in the development of cancer therapeutics directed against the Ras-mitogen-activated protein kinase pathway. Clin. Can. Res. 2008; 14(12): 3651–6.
31. Wang SJ, Li R, Ng TSC, et al. Efficient blockade of locally reciprocated tumor-macrophage signaling using a TAM-avid nanotherapy". Sci. Advances 2020; 6: 21, 1-18.
32. Wellbrock C, Karasarides M, Marais R. The Raf proteins take centre stage. Nat Rev Mol Cell Biol. 2004; 5(11): 875-85.
33. Menzies AM, Long GV, Murali R. Dabrafenib and its potential for the treatment of metastatic melanoma. Drug Des Devel Ther. 2012; 6:391-405.
34. Brummer T, McInnes C. Raf kinase dimerization: implications for drug discovery and clinical outcomes. Oncogene 2020; 39, 4155–4169.
35. Haarberg HE, Smalley KS. Resistance to Raf inhibition in cancer. Drug Discov. Today Technol. 2014; 11:27-32.
36. Hatzivassiliou G, Song K, Yen I. Raf inhibitors prime wild-type Raf to activate the MAPK pathway and enhance growth. Nature Letters 2010; 464(7287):431-435.
37. Oh YT, Deng J, Yue P, et al. Paradoxical activation of MEK/ERK signaling induced by B-Raf inhibition enhances DR5 expression and DR5 activation-induced apoptosis in Ras-mutant cancer cells. Sci Rep. 2016; 6:26803.
38. Dumaz N, Hayward R, Martin J, et al. In Melanoma, Ras Mutations Are

Accompanied by Switching Signaling from BRaf to CRaf and Disrupted Cyclic AMP Signaling. Cancer Res. 2006; (66) (19) 9483-9491.
39. Emuss V, Garnett M, Mason C, et al. Mutations of C-Raf are rare in human cancer because C-Raf has a low basal kinase activity compared with B-Raf. Cancer Res. 2005; 65 (21): 9719–26.
40. Wilhelm SM, Adnane L, Newell P, et al. Preclinical overview of sorafenib, a multikinase inhibitor that targets both Raf and VEGF and PDGF receptor tyrosine kinase signaling. Mol Cancer Ther. 2008; 7 (10): 3129–40.
41. Keating GM, Santoro A. Sorafenib: a review of its use in advanced hepatocellular carcinoma. Drugs 2009; 69 (2): 223–40.
42. Smalley KS, Xiao M, Villanueva J, et al. CRaf inhibition induces apoptosis in melanoma cells with non-V600E BRaf mutations. Oncogene. 2009; 28 (1): 85–94.
43. Nexavar (sorafenib) dosing, indications, interactions, adverse effects, and more. Medscape Reference. WebMD. Accessed June 7, 2021.
44. Nexavar (sorafenib) tablet, film coated [Bayer HealthCare Pharmaceuticals Inc.]. DailyMed. Bayer HealthCare Pharmaceuticals Inc. Nov. 2013. Accessed June 7, 2021.
45. Escudier B, Eisen T, Stadler WM, et al. Sorafenib in advanced clear-cell renal-cell carcinoma. New England Journal of Medicine. 2007; 356 (2): 125–34.
46. ASCO: Sorafenib Halts Resistant Thyroid Cancer. www.medpagetoday.com. Accessed June 7, 2021.
47. Kortum R.L., Morrison D.K. Path Forward for Raf Therapies: Inhibition of Monomers and Dimers. 2015; 28(3) 279-281.
48. Chapman PB, Hauschild A, Robert C, et al. Improved survival with vemurafenib in melanoma with BRAF V600E mutation. New Engl J Med 2011; 364: 2507–2516.
49. https://druginfo.nlm.nih.gov/ drug portal /name/dabrafenib. Accessed June 7, 2021.
50. Gibney GT, Zager JS. Clinical development of dabrafenib in BRaf mutant melanoma and other malignancies. Expert Opinion on Drug Metabolism & Toxicol. 2013; 9(7): 893–9.
51. Flaherty KT, Infante JR, Daud A, et al. Combined BRaf and MEK Inhibition in Melanoma with BRaf V600 Mutations. New England J. Medicine. 2012; 367 (18): 1.
52. Koumaki K, Kontogianni G, Kosmidou V, et al. BRAF paradox breakers PLX8394, PLX7904 are more effective against BRAFV600E CRC cells compared with the BRAF inhibitor PLX4720 and shown by detailed pathway analysis. Biochim Biophys Acta Mol Basis Dis. 2021; 1867(4):166061.
53. Janku F. Interim results from a phase 1/2 precision medicine study of PLX8394 – a next generation BRAF inhibitor. 32nd EORTC-NCI-AACR Symposium on Molecular Targets and Cancer Therapeutics, Oct. 2020.
54. Sommer E, Dry H, Cross D et al. Elevated SGK1 predicts resistance of breast cancer cells to Akt inhibitors. Biochem. J. 2013; 452: 499–508.
55. Wishart DS, Knox C, Guo AC et al. DrugBank: a knowledgebase for drugs, drug actions and drug targets. Nucleic Acids Res 2008; 36: D901-6.
56. Law V, Knox C, Djoumbou Y et al. DrugBank 4.0: shedding new light on drug metabolism. Nucleic Acids Res. 2014; 42(1):D1091-7. 24203711.
57. DataWarrior, a Cheminformatics Program for Data Visualization and Analysis http://www.openmolecules.org/datawarrior/. Accessed June 7, 2021.
58. Ertl P, Rohde B, Selzer P. Fast calculation of molecular polar surface area as a sum of fragment-based contributions and its application to the prediction of drug transport properties. J Med Chem 2000; 43: 3714-3717.
59. Hitchcock SA, Pennington LD. Structure-brain exposure relationships. J Med Chem

2006; 49 (26): 7559–7583. doi:10.1021/jm060642i.

60. Veber DF, Johnson SR, Cheng H-Y et al. Molecular properties that influence the oral bioavailability of drug candidates. J Med Chem 2002; 45(12): 2615-2623.
61. Lipinski CA, Lombardo F, Dominy BW et al. Experimental and computational approaches to estimate solubility and permeability in drug discovery and development settings. Adv Drug Delivery Rev 1997; 23: 4-25.
62. http://www.rcsb.org/pdb/home/home.do. Accessed June 7, 2021.
63. Guex N and Peitsch MC. SWISS-MODEL and the Swiss-PdbViewer: An Environment for Comparative Protein Modeling. Electrophoresis 1997; 18:2714-2723; http://www.expasy.org/spdbv/. Accessed June 7, 2011.
64. ArgusLab 4.0.1, Thompson MA, Planaria Software LLC, Seattle, WA, http://www.arguslab.com/. Accessed June 7, 2021.
65. http://www.molinspiration.com/. Accessed June 7, 2021.
66. Richardson C, Williamson D, Parratt M et al. Triazolo[1,5-a]pyrimidines as novel CDK2 inhibitors: protein structure-guided design and SAR. Bioorg Med Chem Lett. 2006; 16(5): 1353-1357.